Talanta 85 (2011) 282–289

Contents lists available at ScienceDirect

Talanta

journal homepage: www.elsevier.com/locate/talanta

# Molecularly imprinted polymers by reversible addition–fragmentation chain transfer precipitation polymerization for preconcentration of atrazine in food matrices

Shoufang Xu[a,b], Jinhua Li[a], Lingxin Chen[a,*]

[a] Key Laboratory of Coastal Zone Environmental Processes, CAS, Shandong Provincial Key Laboratory of Coastal Zone Environmental Processes, Yantai Institute of Coastal Zone Research, Chinese Academy of Sciences, Yantai 264003, China
[b] Graduate University of Chinese Academy of Sciences, Beijing 100049, China

ARTICLE INFO

*Article history:*
Received 20 January 2011
Received in revised form 17 March 2011
Accepted 24 March 2011
Available online 5 April 2011

*Keywords:*
Molecularly imprinted polymers
Atrazine
Reversible addition–fragmentation chain transfer
Precipitation polymerization

ABSTRACT

Controlled/living free radical polymerization (CLRP) has been accepted as an effective technique in preparation of polymers because of its inherent advantages over traditional free radical polymerization. In this work, reversible addition–fragmentation chain transfer (RAFT) polymerization, the ideal candidate for CLRP, was applied to prepare atrazine molecularly imprinted polymers (MIPs) by precipitation polymerization. The resultant RAFT-MIPs demonstrated uniform spherical shape with rough surface containing significant amounts of micropores, leading to an improvement in imprinting efficiency compared with that of the MIPs prepared by traditional precipitation polymerization (TR-MIPs). The maximum binding capacities of the RAFT-MIPs and TR-MIPs were 2.89 mg $g^{-1}$ and 1.53 mg $g^{-1}$, respectively. The recoveries ranging from 81.5% to 100.9% were achieved by one-step extraction by using RAFT-MIPs for preconcentration and selective separation of atrazine in spiked lettuce and corn samples. These results provided the possibility for the separation and enrichment of atrazine from complicated matrices by RAFT-MIPs.


## 1. Introduction

The family of triazines comprises of the most widely employed herbicides in the world. Atrazine, with better efficiency for control of weeds, is probably the most widely used herbicides of this class. The prolonged utilization of atrazine results in its accumulation in environment and represents a threat to the environment and human health. As an endocrine disruptor, atrazine has high carcinogenicity and mutagenicity, especially after biomagnification [1]. It has been reported that atrazine can cause biological effects of model animals even at much lower the regulated safe dose levels [2]. Analysis of atrazine residues is complicated because of their trace level presence, world-wide distribution and great matrix effects. Therefore, high-efficiency pretreatment procedures and high selective and sensitive analysis methods are urgently required for monitoring the presence and determining the levels of atrazine.

The most frequently used methods for the determination of atrazine are high-performance liquid chromatography (HPLC) [3,4] and gas chromatography (GC) [5,6], which always involves in traditional sample pretreatment procedures, such as solid phase extraction (SPE) and solid phase microextraction (SPME). The main problem associated with traditional sorbents of SPE/SPME is the low selectivity and/or low adsorption capacity. A new type of high efficiency adsorbents, molecularly imprinted polymers (MIPs), owing to high sample load capacity, high selectivity, low cost and easy preparation, have been widely applied for preconcentration and high efficient separation of trace analytes in diverse matrices, such as natural, agricultural and food products and environmental samples [7–10].

MIPs are prepared by copolymerization of functional monomers and cross-linkers in the presence of target analytes which act as template molecule. After removal of template, recognition sites complementary in size, shape, and functionality to the template are formed in the three-dimensional polymer network. The mechanism of MIPs formation mainly includes free-radical polymerization and sol–gel process; the former is the more popular, typically including bulk polymerization, suspension polymerization [11], emulsion polymerization [12], and precipitation polymerization [13]. Up to now, bulk polymerization and suspension polymerization have been used for the preparation of MIPs for the determination of triazines [14–16]. However, the resulting MIPs are associated with some problems, involving complicated after-treatment workup, heterogeneous binding sites and slow mass transfer, etc., which restrict its imprinting capacity and extraction efficiency. Recently, controlled/living free radical polymerization (CLRP), has been widely utilized to synthesize MIPs,

* Corresponding author. Tel.: +86 535 2109130; fax: +86 535 2109130.
*E-mail address:* lxchen@yic.ac.cn (L. Chen).

0039-9140/$ – see front matter © 2011 Elsevier B.V. All rights reserved.
doi:10.1016/j.talanta.2011.03.060

including reversible addition–fragmentation chain transfer (RAFT) polymerization, metal-catalyzed atom transfer radical polymerization (ATRP), nitroxide-mediate polymerization (NMP) and iniferter, due to their intrinsic advantages over conventional free radical polymerization, such as producing well-defined polymers with predictable molecular, low polydispersity, controlled composition and functionality [17]. RAFT polymerization, the ideal candidate for CLRP has also been applied for MIPs preparation because of its versatility and simplicity. For example, Titirici and Sellergren [18] have prepared L-phenylalanine anilide imprinted core-shell microspheres by RAFT polymerization on silica beads. The usage of RAFT prevented visible gel formation. Subsequently, the same approach was exploited by Lu and coworkers [19]. They immobilized chain transfer agent on silica nanoparticles and synthesized 2,4-dichlorophenoxyacetic acid imprinted microspheres by surface RAFT polymerization. The forming of uniform MIP shells with adjustable thicknesses can be attributed to the intrinsic characteristics of RAFT polymerization. Pan and coworkers [20] have proved that MIPs prepared by RAFT precipitation polymerization (RAFT-MIPs) possess improved binding capacity and larger binding constant than MIPs prepared by traditional precipitation polymerization (TR-MIPs).

In this work, the development of RAFT precipitation polymerization for the preparation of atrazine MIPs with higher imprinting efficiency and binding capacity was described. To the best of our knowledge, this was the first demonstration for the preconcentration of atrazine in food matrix using RAFT-MIPs. Some variable parameters influencing the final characteristics of the obtained materials in terms of capacity, affinity and selectivity for target analyte, such as the nature of functional monomers, cross-linkers and solvent, the amount and the nature of chain transfer agent (CTA) were investigated in detail. The performances of RAFT-MIPs for extraction of atrazine in spiked lettuce and corn samples were also evaluated.

## 2. Experimental

### 2.1. Reagents

Bromobenzene, magnesium, benzyl bromide, tetrahydrofuran (THF), carbon disulfide, 2-chloropropane and petroleum ether were purchased from Shanghai Chemical Reagents Company (Shanghai, China). Methacrylic acid (MAA), 4-vinlpyridine (4-VP), ethyleneglycol dimethacrylate (EGDMA), trimethylolpropane trimethacrylate (TRIM) and divinylbenzene (DVB) were purchased from Sigma–Aldrich and distilled in vacuum prior to use in order to remove stabilizers. 2,2′-azo-bis-isobutyronitrile (AIBN) were purchased from Shanghai Chemical Reagents Company and recrystallized in methanol prior to use. Acrylamide (AAm) was purchased from Tianjin Reagent Plant (Tianjin, China) and recrystallized in water prior to use. Atrazine, simetryn, simazine, prometryne, and ametryn were kindly provided by Binzhou Agricultural Technology Co., Ltd. (Shandong, China). Furazolidone and carbendazim were purchased from J&K Technology Limited (Beijing, China). The individual stock solutions (200 mg $L^{-1}$) were prepared in acetonitrile (ACN) and stored at −18 °C in the dark. All other reagents were used as supplied without a further purification step.

### 2.2. Synthesis of chain transfer agent (CTA)

CTA was synthesized as reported [21]. Briefly, magnesium offals (1.5 g), bromobenzene (0.5 mL), a grain of iodine and 20.0 mL absolutely dry THF were introduced into a three-necked flask under nitrogen atmosphere. Bromobenzene (4.8 mL) in THF (15.0 mL) was added dropwise with stirring until the brown of iodine disappeared. The reaction mixture was left to stand for 8 h to ensure the complete reaction of bromobenzene. When the reaction solution was cooled down till room temperature, carbon disulfide (4.0 mL) in THF (20.0 mL) was added dropwise, and the reaction was kept at that temperature for 4 h. Benzyl bromide (12.0 mL) was then added, and the reaction mixture was heated to 50 °C and kept for 3 h. After cooling to room temperature, the solution was poured into 100.0 mL water, and extracted by petroleum ether, followed by collecting and concentrating the organic phase. The residue was purified by chromatography using petroleum ether to yield CTA **1** which is cardinal liquid. Bright yellow liquid CTA **2** was synthesized according to the same procedure described above but using 2-chloropropane substitute for bromobenzene.

### 2.3. Preparation of RAFT-MIPs

Atrazine imprinted polymers were prepared by RAFT precipitation polymerization, according to the non-covalent approach, using MAA as functional monomer, EGDMA as cross-linker and ACN as porogens. Briefly, prior to polymerization, pre-polymer solution was prepared by dissolving MAA (2 mmol) and atrazine (0.5 mmol) in ACN (30 mL) and was stored at 4 °C in dark for 12 h. Then, EGDMA (10 mmol), AIBN (20 mg), and CTA (60 μL) were added to the pre-polymer solution. The solution was degassed by ultrasonic bath for 5 min, and then purged with nitrogen for 10 min while cooling on an ice bath before being sealed. Polymerization was performed in water bath at 40 °C for 2 h, followed by 60 °C for 24 h. The resultant polymer particles were separated from the reaction mixture and washed with methanol/acetic acid solution (9:1, v/v) to remove both the template molecules and residual monomers. Finally, the particles were dried to constant weight under vacuum at 40 °C. For comparison, MIPs were prepared by traditional precipitation polymerization (TR-MIPs) in the same manner but without the addition of CTA. As control, non-imprinted polymers (NIPs) were prepared under identical conditions but omitting the template in the reaction system. Scheme 1a shows the chemical structures of CTA **1** and CTA **2**, atrazine, EDGMA, AIBN and MAA.

### 2.4. Characterization of imprinted particles

The morphology of the MIPs was examined by scanning electron micrography (SEM, JSM 5600 LV, operating at 20 kV). All samples were sputter-coated with gold before SEM analysis.

The adsorption experiments were carried out as follows: 20.0 mg polymer particles were dispersed in 5 mL flask containing 2.00 mL atrazine solution of various concentrations. After shaking for 24 h at room temperature, the samples were centrifuged and the supernatant solution was collected, concentrations of which were determined using HPLC–UV. The amount of atrazine adsorbed onto the polymer ($Q$) was determined according to the following formula:

$$Q = \frac{(C_0 - C_F)V}{m}$$

where $C_0$ (mg $mL^{-1}$) and $C_F$ (mg $mL^{-1}$) are the initial and final atrazine solution concentrations, respectively. $V$ (mL) is the sample volume and $m$ (g) is the mass of the polymer. The tests were done in triplicate.

### 2.5. Sample preparation and HPLC–UV analysis

Lettuce and corn samples were prepared as reported [16,22]. Briefly, the edible parts of fresh lettuce and corn were taken and crushed into homogenate, then 50 mL ACN was added into 50 g homogenates and incubated for 8 h before filtering. The filtrate was extracted with dichloromethane and evaporated to dryness. The

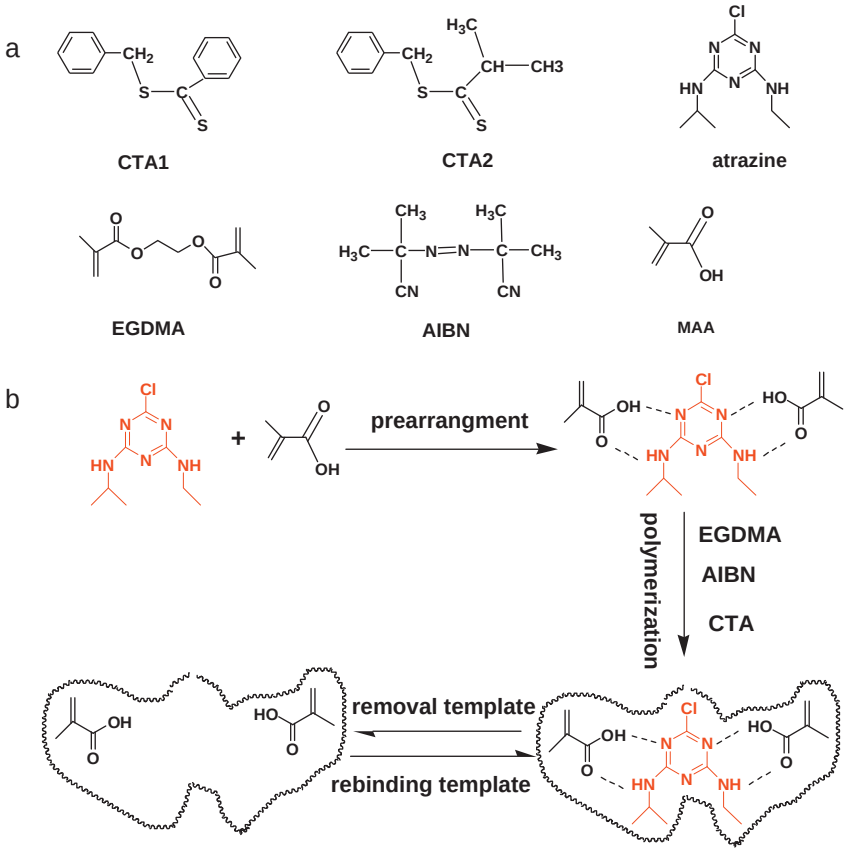


**Scheme 1.** Structures of chemicals (a) and preparation process schematic of atrazine imprinted polymers by RAFT precipitation polymerization (b). For CTA **1**: **R** = $C_6H_5CH_2$–; **Z** = $C_6H_5$–. For CTA **2**, **R** = $C_6H_5CH_2$–; **Z** = $(CH_3)_2CH$–.

residue was redissolved in ACN. For spiked samples, appropriate amounts of atrazine standards were added into the ACN solution, at two levels: 10 μg $L^{-1}$ and 100 μg $L^{-1}$.

RAFT-MIPs of 100 mg were dispersed in 5 mL blank or spiked sample solution prepared above, and incubated for 1 h at room temperature before being collected by a 0.22 μm microporous membrance. The RAFT-MIPs were washed with 3 mL methanol to reduce nonspecific adsorption, and then eluted with 5 mL desorption solvent (methanol/acetic acid, 9:1, v/v). The desorption solution was dried and redissolved in 200 μL ACN, and then analyzed with HPLC instrument (Skyray Instrument Inc., Kunshan, China). A C18 column (Arcus EP-C18, 5 μm, 4.6 mm × 250 mm Column, Exformma Technologies, USA) was used as the analytical column. HPLC conditions employed for this work were as follows: mobile phase, acetonitrile/water (70:30, v/v); flow rate, 1.0 mL $min^{-1}$; room temperature; UV detection, at 220 nm; injection volume, 20 μL. For comparison, 100 mg TR-MIPs were employed to perform the same extraction and analysis procedure as the RAFT-MIPs.

## 3. Results and discussion

### 3.1. RAFT precipitation polymerization for preparation of MIPs

The imprinting process of RAFT polymerization for atrazine is illustrated in Scheme 1b. Homogeneous morphology and excellent recognition properties are the most significant indicators of well functioning MIPs, which are mainly the result of optimization of typical factors such as type and proportion of porogens, monomers and cross-linkers. Especially, for the proposed RAFT precipitation polymerization, the unique factor, CTA, is also considered.

#### 3.1.1. Porogens

It is essential that there is an adequate match between the polarity of the porogen and the solubility parameters of the developing polymer, in order to obtain the MIPs with permanent pore structures and highly uniform particle size [13]. Porogens with low solubility undergoes phase separation early and tend to form larger pores and materials with lower surface areas, while porogens with higher solubility phase separate later in the polymerization, which provides materials with smaller pores size with higher surface area. The aprotic and low polar organic solvents, typically toluene, ACN and chloroform, were tested as polymerization solvents. When using chloroform as porogen, the polymerization solution was gel-like, while soft and sheet-like structure was obtained by using toluene. Using ACN as porogen, the highest binding capacity and most uniform morphology was obtained. So, ACN was employed as porogen for the present RAFT polymerization studies.

#### 3.1.2. Monomers

Stronger interaction between templates and monomers is crucial for producing highly stable complex, and thereby higher recognition specificity of the MIPs [23]. Therefore, tailoring of a functional monomer to the template molecules is the most important step in molecular imprinting process. Three commonly used monomers, MAA, AAm and 4-VP were tested in the MIPs preparation, respectively. The resulting shape of particles were sheet-like aggregations when AAm was used, while fine particles with diameter about 100 nm formed using 4-VP as monomer, both of which were hard to be used for separation. The highest binding capacity of the MIPs was obtained by using MAA as functional monomer; therefore MAA was selected as the optimal monomer. The result was expected and in consistent with former experi-

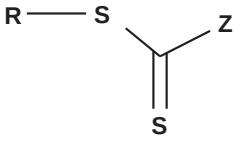


**Fig. 1.** General molecular structure of CTA with dithioester structure. **R** is a free radical leaving group, and **R** free radical must be able to reinitiate polymerization; the role of **Z** is to modify addition or fragmentation rate.

mental results [24,25]: MAA displayed the best effectiveness as functional monomer when used to imprinting atrazine because they can form double hydrogen bond with atrazine, which leads to an understanding that a functional monomer is required to have both strong binding and multiple binding capacity.

### 3.1.3. Cross-linkers

Cross-linkers play a vital role in the recognition property of MIPs because they control network structure of MIPs [7]. EGDMA, TRIM and DVB were introduced for cross-linkers selection. Using DVB led to the lowest imprinting yields. Higher binding capacity was gained by using EGDMA when compared to TRIM. Therefore, EGDMA was chosen as the cross-linkers in the following MIPs preparation.

### 3.1.4. Chain transfer agent (CTA)

Besides the generally optimized polymerization factors mentioned above, chain transfer agent (CTA) is quite critical for RAFT polymerization for preparing MIPs. Fig. 1 shows the common structure of CTA with dithioester. An ideal CTA should satisfy the following requirements [26]: CTA should have a high chain transfer constant; the **R–S** bond should be a weak single bond because **R** is a free radical leaving group, and **R** free radical must be able to reinitiate polymerization, and furthermore, the activity of **R** free radical should be higher than primary free radical; the role of **Z** is to modify addition or fragmentation rate.

Two kinds of CTAs were synthesized (Scheme 1a) and employed for the proposed atrazine MIPs, which were differed in **Z** group. Under the optimum conditions, the MIPs using CTA **1**, namely RAFT-MIP1, exhibited better uniformity and more spherical shape (Fig. 2a), and therefore higher binding capacity, which could be attributed to the fact that CTA **1** had the higher reactivity than CTA **2**, which is in accordance with the reported trend, where CTA had higher reactivity when the **Z** group was a conjugated group, such as phenyl group or naphthyl [27].

In addition to the structure of CTA, the stoichiometric ratios also have profound impact on RAFT polymerization. The concentration of free radical in entire system can be maintained constant on the condition that the concentration of chain propagation is much lower than that of CTA [28]. So, the concentration effect of CTA **1** was also investigated. Increasing the amounts of CTA **1** from 3.3 mM to 10.0 mM, the resultant MIPs particles changed from irregular to spherical shape, and correspondingly the imprinting capacity increased. However, higher volume of CTA resulted in serious polymerization retardation [29]. Finally, 10.0 mM CTA **1** was adopted for RAFT polymerization for further work.

## 3.2. Characterization of MIPs

SEM images of the atrazine MIPs/NIPs are shown in Fig. 2. Under the optimized RAFT polymerization conditions, uniform and spherical particles with a rough surface containing many micropores were obtained (Fig. 2a), which greatly facilitated the adsorption of template molecules. Using CTA **2**, the obtained imprinted particles were globular with a smooth surface but with a broader size distribution (1.25–3.42 μm), shown in Fig. 2b. As seen clearly from Fig. 2c, the irregular MIPs aggregates were obtained by traditional

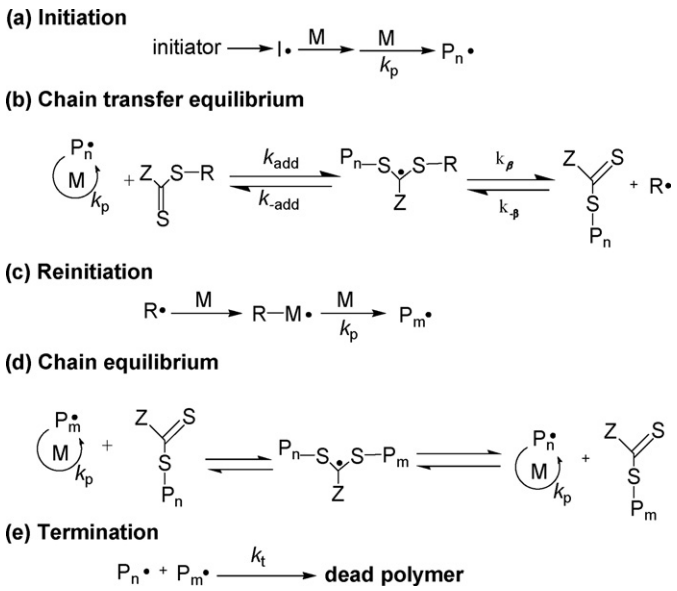


**Scheme 2.** Mechanism of RAFT polymerization. Adapted from Ref. [30].

precipitation polymerization and only a small number of particles were monodispersed, which resulted in the incomplete template removal, small binding capacity, and slow mass transfer. For the control polymers, those NIPs have the similar morphology to the corresponding MIPs, as seen in Fig. 2(d)–(f). The SEM images provided support for the results of binding experiment.

In precipitation polymerization, growing polymer chains do not overlap or coalesce but continue to grow individually by capturing newly formed oligomers and monomers in diluted reaction system, and then separate from the solution with micro spherical morphologies. Ascribed to the mechanism of traditional free radical polymerization, the microstructure, degree, and polydispersity of the obtained polymers are uncontrollable. The existence of irreversible chain transfer reaction resulted in several small globular particles, which were aggregated into one bigger irregular particle, as seen from Fig. 2c. The mechanism of RAFT polymerization first proposed by Rizardo [30] (Scheme 2), has been widely accepted in recent years. The core of the mechanism consists of chain transfer equilibrium and chain equilibrium: chain propagation free radical reacts with CTA, which results in the original free radical formation of dormant polymer, and CTA generating new radicals. Those processes are reversible, so the concentration of free radical in entire system can be maintained constant, and therefore the desired "living" polymerization can be achieved. Thanks to the intrinsic advantages of "living" polymerization, the lifetime of the growing radical can be controlled, resulting in the synthesis of polymer chains with predefined molar mass, low polydispersity, and controlled composition, displaying uniform and spherical particles in the morphology of imprinted polymers. Different structures of CTA result in different capability for living polymerization, so there are some differences in the morphology of imprinted polymers (Fig. 2).

## 3.3. Adsorption analysis and recognition mechanism

The adsorption isotherm experiments were carried out using atrazine at concentrations in the range of 10–80 mg $L^{-1}$. As shown in Fig. 3, for the four kinds of polymers, binding capacity increased quickly and continuously along with the increase of initial concentration; at higher equilibrium concentration than 60 mg $L^{-1}$, binding capacity became stable. This was a common and normal

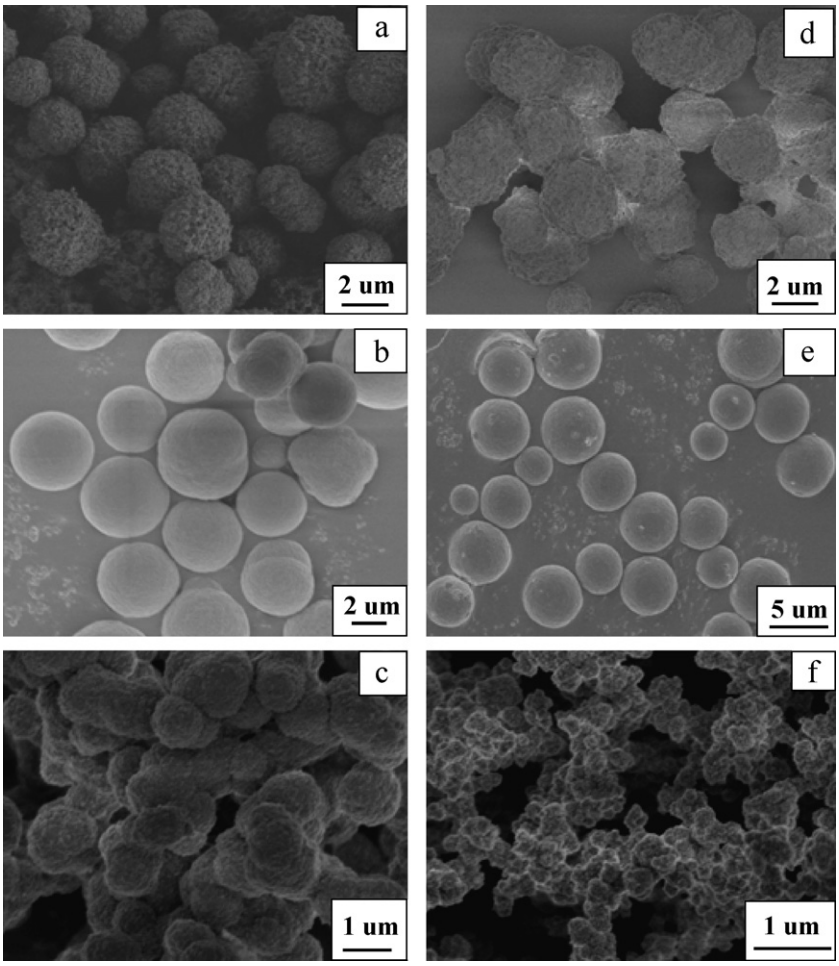


**Fig. 2.** SEM images of MIPs and the corresponding NIPs prepared by RAFT precipitation polymerization in the presence of CTA **1** (a, d); CTA **2** (b, e); and prepared by traditional precipitation polymerization (c, f).

phenomenon for the static adsorption experiment, which can be explained as follows. There was an adsorption–desorption equilibrium between MIPs and initial template solution. When the initial solution concentration is low, the adsorbed template amount is low, which cannot occupy all of the recognition sites. So, with the increase of initial concentration, more and more recognition sites were utilized, until completely saturated.

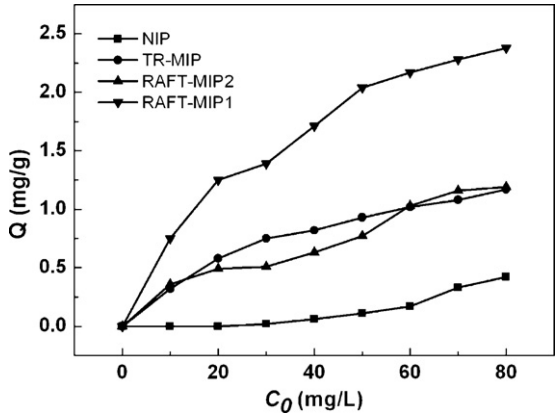


**Fig. 3.** Binding isotherms of MIPs and NIPs (in presence of CTA **1**) for atrazine in acetonitrile. Experimental conditions: volume, 2.0 mL; mass of polymer, 20 mg; adsorption time, 24 h.

The obtained RAFT-MIP1 exhibited the highest binding capacity for the template, which can be explained from the SEM characterization (Fig. 2a). The presence of vast micropores in RAFT-MIP1 particles paved the way for atrazine entering into the binding bites located in the interior of polymer particles, improving the utilization of recognition sites. High specific surface area, attributed to the rough surface, provided facility for adsorbing template molecules. The values of TR-MIPs were similar to that MIPs prepared by RAFT precipitation polymerization with CTA **2** (RAFT-MIP2). The reason for the phenomenon could be found from the SEM photographs (Fig. 2). For TR-MIPs, the polymer particles aggregated into irregular big ones, and most of the imprinted binding sites were located in the interior of highly cross-linked polymers, so it was quite difficult for atrazine entering into the binding bites, which reduced the binding capacity for target analytes. That could answer for the reason why the binding capacity of TR-MIPs was much lower than that of RAFT-MIP1. For RAFT-MIP2, the imprinted polymer particles were monodispersed, however their surfaces were smooth, which were unfavorable for target adsorption. There were no selective recognition sites in NIPs, so the binding capacity was the lowest (Fig. 3). Taking into account the results above, RAFT-MIP1 was chosen for latter selectivity binding experiment and spiked sample analysis.

Scatchard analysis was employed to further evaluate the molecular recognition properties of imprinted polymers. The Scatchard equation is expressed as,

$$\frac{Q}{C_e} = \frac{Q_{\max}}{K_d} - \frac{Q}{K_d}$$

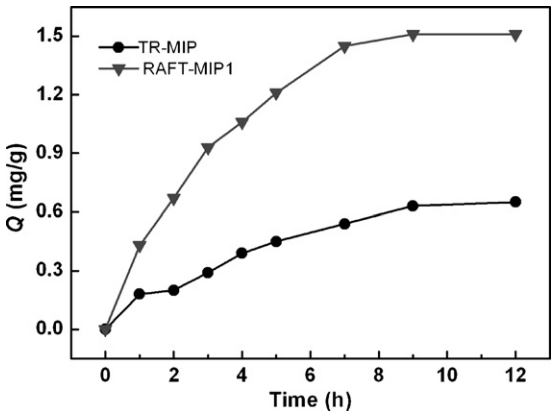


**Fig. 4.** Kinetic uptakes of atrazine molecules onto RAFT-MIP1 and TR-MIP. Experimental conditions: initial concentration of the compounds, $C_0 = 40\,mg\,L^{-1}$. Other experimental conditions were the same as those described in Fig. 3.

where $Q$ stands for the binding capacity ($mg\,g^{-1}$) of atrazine on polymer, $K_d$ represents the equilibrium dissociation constant ($mg\,L^{-1}$), $Q_{max}$ ($mg\,g^{-1}$) is the theoretical maximum adsorption amounts of template molecule on polymers, and $C_e$ ($mg\,mL^{-1}$) is the equilibrium concentration of atrazine in the solution. According to the slope and intercept of the Scatchard plot, namely the relationship between $Q/C_e$ and $Q$, $K_d$ and $Q_{max}$ can be calculated. For RAFT-MIP1, $K_d$ and $Q_{max}$ were calculated to be $0.0136\,mg\,L^{-1}$ and $2.89\,mg\,g^{-1}$, respectively, whereas the values for TR-MIPs were $0.026\,mg\,L^{-1}$ and $1.53\,mg\,g^{-1}$, respectively, which was consistent with the experimental observation. However, the $K_d$ value was different from the old paper by Mosbach's group ($10^{-6}$ M) [25] and Takeuchi's group (12 μM)[31]. Perhaps, this phenomenon can be explained as follows: (1) the preparation methods were different. In the old paper, irregular MIP particles with size about 25 μm were prepared by bulk polymerization; in this work, sphere particles with size of 3 μm were prepared by RAFT precipitation polymerization; (2) the solvents were different: ACN was used in this work while toluene was used in the old paper. Maybe the polarity of the solvent can influence the value. Combined with the SEM images (Fig. 2), it can be concluded that the monodispersed and spherical particles with a rough surface favor the higher binding capacity.

Fig. 4 shows the time dependent evolutions of the atrazine amount bound by the RAFT-MIP1 and TR-MIP, respectively. It was observed that the adsorption amounts of atrazine onto both RAFT-MIP1 and TR-MIP increased with time. However, RAFT-MIP1 offered the more rapid adsorption for atrazine from solution phase than the latter. The RAFT-MIPs took up 50% of the equilibrium adsorption amount during 2.5 h and nearly reached saturation state within 7 h, while the TR-MIPs needed 9 h to reach adsorption equilibrium. And, more importantly, to attain the same adsorption capacity (the equilibrium adsorption capacity of TR-MIPs), RAFT-MIPs required only one fifth of time required by TR-MIPs, indicating that the RAFT polymerization is an effective way to create a polymer with better mass transfer properties; in the same adsorption time, the adsorption capacity of RAFT-MIPs is about 2–3 times higher of TR-MIPs. This can be attributed to those micropores on the surface of RAFT-MIPs, which provide more accessible recognition sites. Therefore, the RAFT polymerization method is quite applicable for MIP preparation and the RAFT-MIPs as excellent sorbent could be widely applied in the SPE field.

### 3.4. Molecular selectivity of MIPs

To investigate the binding specificity of the RAFT-MIPs, selectivity test was carried out by using the structural analogues including ametryn, propazine, simetryn, simazine, and other two herbicide, carbendazim and furazolidone as control compounds. It can be seen from Table 1, that the adsorption capacity of NIPs is very close for the seven compounds since there are not selective recognition sites in NIPs and the adsorption for those compounds are all non-selective. Both the RAFT-MIPs and TR-MIPs exhibited high selectivity for triazines derivatives than other structurally unrelated compounds. This result was expected because the triazine herbicides have very similar structures and even antibodies have difficulty distinguishing between them. Moreover, the obtained MIPs exhibited higher binding affinity for atrazine compared to all the other tested triazines. Close analysis of the binding data demonstrates that the level of cross-reactivity is roughly proportional to the structure resemblance to the imprinted species. The observed selectivity for the triazines was presumably caused by the template effects. As reported [31] in addition to the side chain amino groups of atrazine play important roles in the recognition process, the chloro group also seems to be important for molecular recognition. And the binding affinity for triazines was decreases in the rank order $-Cl > -OCH_3 > -OH > -SCH_3$. However, propazine was a special case, as can be seen from Table 1. This phenomenon also can be seen from a former paper about atrazine MIPs [16]. This may be attributed to the solvent used in the preparation process [24]: solvents also engaged as templates during the imprinting process and affected the binding ability of resultant polymers, and solvent effects on the resultant selectivity have been reported by Hosoya [32]. However the mechanism was unknown now. For NIPs, the nonspecific binding is higher for more polar compounds. This phenomenon can be attributed to the presence of carboxylic acid groups on the polymer surface, which can be involved in hydrogen bonding with polar molecules [25]. The recognition mechanism could be explained as follow: in preparation process, many specific recognition sites with respect to template were generated in imprinted polymers, so the template could strongly bound to the polymers in binding process. Although the same hydrogen bond could be formed between the analogues and functional monomers because of the similar structure with template molecule, adsorption capacity was much lower than that of template molecule (Table 1). The result indicated that the recognition property of MIPs was not only based on the hydrogen interaction between template and functional monomers, but also on the complementary match of "cavity" (site) with template in size and shape. The binding capacity of RAFT-MIPs for those five triazines was higher than that of TR-MIPs, respectively, which was consistent with the binding observation and SEM characterization. The selectivity factors of RAFT-MIPs were higher than those of TR-MIPs, which can be attributed to the fact that RAFT polymerization can generate more homogeneous binding cavities when compared to traditional free radical polymerization.

### 3.5. Analysis of atrazine in food samples

To evaluate the applicability of RAFT-MIPs in selective preconcentration and separation of atrazine, recover was investigated by spiking the atrazine standards into the lettuce and corn samples at two concentrations ($10\,\mu g\,L^{-1}$ and $100\,\mu g\,L^{-1}$), and each concentration was analyzed five replicates, respectively. Typical atrazine chromatographic peak of the lettuce and corn samples are shown in Fig. 5 and Table 2, and TR-MIPs were used for comparison. No interferences of endogenic compounds are observed at the elution zone of atrazine, and the remarkable signal enhancements were obtained by RAFT-MIPs extraction (Fig. 5a), which could be attributed to that fact RAFT-MIPs have much higher imprinting efficiency than those TR-MIPs, so the matrix effects could be drastically reduced and the atrazines could be preconcentrated. It was extremely difficult to detect the atrazine without performing the

**Table 1**
Imprinting efficiency and selectivity coefficient of the imprinted polymer beads.

| Compound | Traditional precipitation polymerization | | | | RAFT precipitation polymerization | | | |
|---|---|---|---|---|---|---|---|---|
| | $Q$ (mg g$^{-1}$) | | $\alpha$[a] | $\beta$[b] | $Q$ (mg g$^{-1}$) | | $\alpha$ | $\beta$ |
| | MIP | NIP | | | MIP | NIP | | |
| Atrazine | 0.82 | 0.12 | 6.8 | – | 1.5 | 0.14 | 10.8 | – |
| Ametryn | 0.38 | 0.10 | 3.8 | 1.8 | 0.98 | 0.23 | 4.3 | 2.5 |
| Propazine | 0.39 | 0.08 | 4.9 | 1.4 | 0.63 | 0.13 | 4.9 | 2.2 |
| Simetryn | 0.48 | 0.10 | 4.8 | 1.4 | 0.71 | 0.29 | 2.4 | 4.4 |
| Simazine | 0.64 | 0.11 | 5.8 | 1.2 | 1.2 | 0.16 | 7.7 | 1.4 |
| Carbendazim | 0.08 | 0.06 | 1.3 | 5.1 | 0.12 | 0.07 | 1.7 | 6.3 |
| Furazolidone | 0.09 | 0.07 | 1.3 | 5.3 | 0.11 | 0.09 | 1.2 | 8.8 |

[a] Imprinting factor, $a = Q_{MIP}/Q_{NIP}$. $Q_{MIP}$ and $Q_{NIP}$, adsorption capacity of the template or the analogues on MIP and NIP, respectively.
[b] Selectivity factor, $\beta = a_{tem}/a_{ana}$. $a_{tem}$ and $a_{ana}$, imprinting factor toward the template molecule and the analogue, respectively

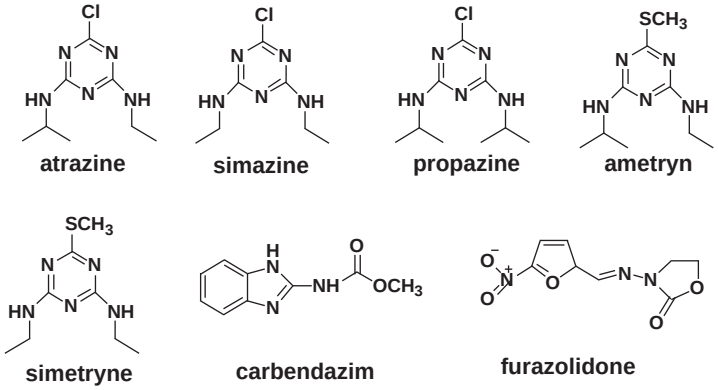


Chemical structures of compounds used in selective experiments

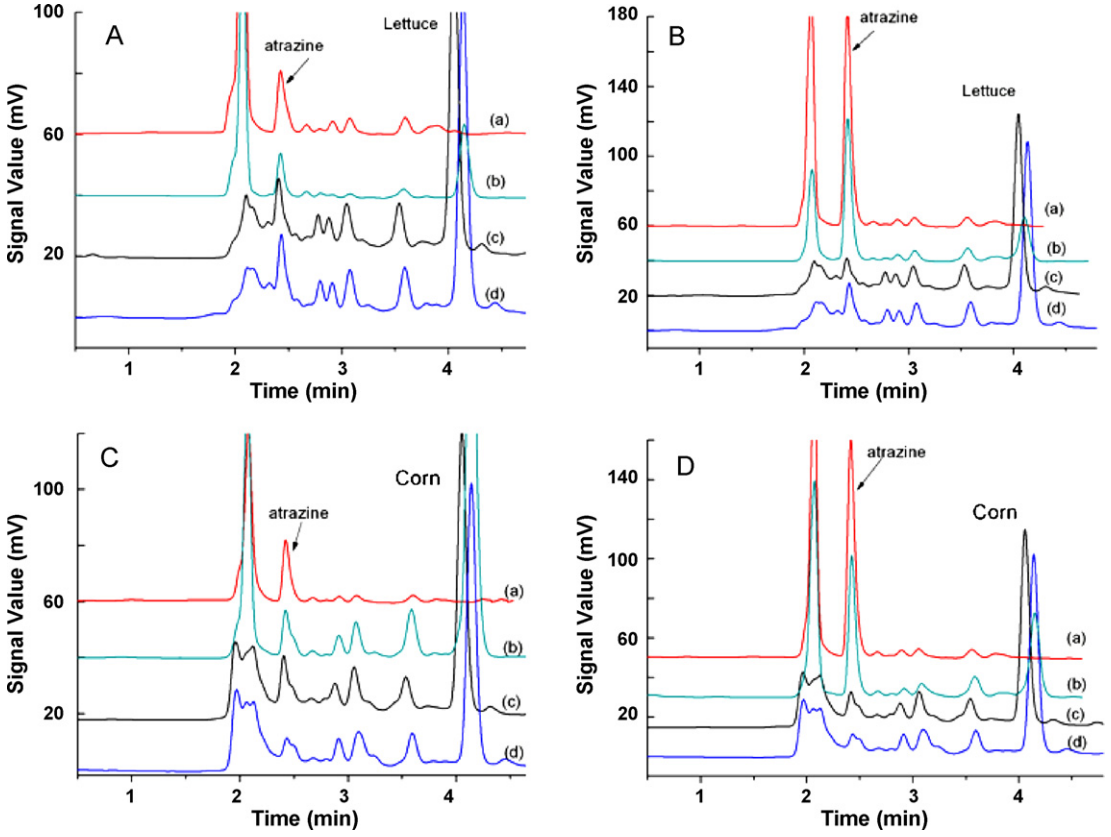


**Fig. 5.** Chromatograms of atrazine at 10 μg L$^{-1}$ in spiked lettuce sample (A) and corn sample (C), 100 μg L$^{-1}$ in spiked lettuce sample (B) and corn sample (D): extracted with RAFT-MIPs (a) and TR-MIPs (b), and without extraction (c), and unspiked samples extracted with RAFT-MIPs (d).

**Table 2**
Recoveries and precision of atrazine in spiked sample ($n = 5$).[a]

| Samples | Initial concentration ($\mu g\,L^{-1}$) | Spiked level ($\mu g\,L^{-1}$) | Recovery (%) | | RSD (%) | |
|---|---|---|---|---|---|---|
| | | | RAFT-MIP | TR-MIP | RAFT-MIP | TR-MIP |
| Lettuce | 2.68 | 10 | 100.9 | 80.5 | 5.6 | 8.3 |
| | | 100 | 89.9 | 72.3 | 7.2 | 9.8 |
| Corn | 1.39 | 10 | 95.6 | 86.2 | 9.3 | 10.5 |
| | | 100 | 81.5 | 67.8 | 4.9 | 7.6 |

[a] Experimental conditions: 5 mL spiked solutions; 100 mg RAFT-MIPs; wash solution, 3 mL methanol; elution solution, 5 mL methanol/acetic acid, 9:1, v/v; redissolved solution, 200 μL ACN.

extraction preparation process (Fig. 5c), because of the low concentration level and severe interferences from complicated matrices. As for the blank samples extracted by RAFT-MIPs, it can be seen that one peak with low intensity appeared at *ca.* 2.4 min (Fig. 5d), which can be assigned to endogenous atrazine present in the lettuce and corn samples since its retention time corresponded to that of the standard.

The calibration curve for the detection of atrazine were obtained by performing a linear regression analysis ranging from 0.05 to 50 mg/L. Good linearity was obtained with correlation coefficients of $R > 0.9999$. The limits of determinations (LOD) was 2.8 μg/L based on a signal-to-noise ratio of 3. Precision was calculated in term of intraday repeatability ($n = 6$) and interday reproducibility (6 different days) on 0.1 mg/L. The intraday repeatability evaluated as RSD was 3.2%, and the interday reproducibility was 4.1%. Averaged recoveries from 89.9% to 100.9% were obtained for atrazine spiked lettuce samples by using RAFT-MIPs, with the precisions between 5.6% and 7.2%, while the recoveries between 72.3% and 80.5% and the precisions within 8.3% and 9.8% were obtained by using TR-MIPs (Table 2). Higher recoveries and precisions are based on the higher imprinting efficiency, which is facilitated by amounts of effective sites of the RAFT-MIPs. Meanwhile, in corn sample, higher recoveries and precisions were obtained by RAFT-MIPs for spiked atrazine analysis (Table 2). The results demonstrated that the atrazine imprinted polymers prepared by RAFT polymerization had higher selectivity and enrichment ability. Hence, the RAFT-MIPs for atrazine offer a simple and robust method for direct analysis of atrazine from complicated food samples.

In addition to as solid-phase extraction sorbent for preconcentration of samples before determination using traditional methods, another potential use of the obtained atrazine RART-MIPs is as sorbent for removal of triazines in environmental treatment. When the adsorption equilibrium is achieved, the sorbent maybe regenerated and reused. The RAFT-MIPs presented here can be considered as a potential alternative to those sorbent used in environmental clean-up application.

## 4. Conclusions

An alternative general method was presented to prepare atrazine MIPs by RAFT precipitation polymerization. The resultant RAFT-MIPs exhibited excellent characteristics, such as highly spherical and uniform morphology, higher binding capacity and selectivity for atrazine. The analytical method based on RAFT-MIPs was successfully applied for atrazine analysis in spiked lettuce and corn samples. Given the advantages of "living polymerization" of the RAFT polymerization method, we expect it can be further employed for preparing the atrazine or other target MIPs with controllable core–shell nanoparticles and thereby offering more recognition sites and higher imprinting efficiency. And then the obtained MIPs will be applied for food and environmental field analysis, where the targeted compounds are present at low levels in complicated matrices, and extended for rapid and accurate quality monitoring in the future.

Though RAFT-MIPs take some advantages over TR-MIPs, more work is still requires to solve the problem of slow mass transfer. Hence, higher binding capacity and quicker mass transfer would be expected by using nano-sized core-shell imprinted polymers and imprinted porous polymers.

## Acknowledgements

Financial support from the National Natural Science Foundation of China (20975089), the Chinese Academy of Sciences (KZCX2-EW-206), Department of Science and Technology of Shandong Province of China (2008GG20005005), the 100 Talents Program of the Chinese Academy of Sciences, and the Department of Science and Technology of Yantai City of China (2010158) is gratefully acknowledged.

## References

[1] L.Z. Zhu, X.F. Cai, J. Wang, J. Environ. Sci. 17 (2005) 748.
[2] J. Kaiser, Science 290 (2000) 695.
[3] R. Zhao, J. Yuan, T. Jiang, J. Shi, C. Cheng, Talanta 76 (2008) 956.
[4] Y.N. Li, H.L. Wu, X.D. Qing, Q. Li, S.F. Li, H.Y. Fu, Y.J. Yu, R.Q. Yu, Anal. Chim. Acta 678 (2010) 26.
[5] B.A. Tomkins, R.H. llgner, J. Chromatogr. A 972 (2002) 183.
[6] L. Bohuss, J. Bozóki, K. Barkáca, G. Záray, Microchem. J. 74 (2003) 165.
[7] X.L. Song, J.H. Li, J.T. Wang, L.X. Chen, Talanta 80 (2009) 694.
[8] C. Long, Z. Mai, Y. Yang, B. Zhu, X. Xu, L. Lu, X. Zou, J. Chromatogr. A 1216 (2009) 2275.
[9] S.F. Xu, J.H. Li, L.X. Chen, J. Mater. Chem. 21 (2011) 4346.
[10] L.X. Chen, S.F. Xu, J.H. Li, Chem. Soc. Rev., 2011. doi:10.1039/C0CS00084A.
[11] T. Jing, X. Gao, P. Wang, Y. Wang, Y. Lin, X. Hu, Q. Hao, Y. Zhou, S. Mei, Anal. Bioanal. Chem. 393 (2009) 2009.
[12] C.J. Tan, H.G. Chua, K.H. Ker, Y.W. Tong, Anal. Chem. 80 (2008) 683.
[13] J. Wang, P.A.G. Cormack, D.C. Sherrington, E. Khoshdel, Angew. Chem. Int. Ed. 42 (2003) 5336.
[14] E. Turiel, A. Martín-Esteban, P. Fernández, C. Pérez-Conde, C. Cámara, Anal. Chem. 73 (2001) 5133.
[15] L. Amalric, C. Mouvet, V. Pichon, S. Bristeau, J. Chromatogr. A 1206 (2008) 95.
[16] Y. Zhang, R. Liu, Y. Hu, G. Li, Anal. Chem. 81 (2009) 967.
[17] H. Wang, W. Zhou, X. Yin, Z. Zhuang, H. Yang, X. Wang, J. Am. Chem. Soc. 128 (2006) 15954.
[18] M.M. Titirici, B. Sellergren, Chem. Mater. 18 (2006) 1773.
[19] C.H. Lu, W.H. Zhou, B. Han, H.H. Yang, X. Chen, X.R. Wang, Anal. Chem. 79 (2007) 5457.
[20] G. Pan, B. Zu, X. Guo, Y. Zhang, C. Li, H. Zhang, Polymer 50 (2009) 2819.
[21] J. Meijier, P. Vermeer, L. Brandsma, Recl. Trav. Chim., Pays-Bas 92 (1973) 601.
[22] Q. Lu, X. Chen, L. Nie, J. Luo, H. Jiang, L. Chen, Q. Hu, S. Du, Z. Zhang, Talanta 81 (2010) 959.
[23] J.F. He, Q.H. Zhu, Q.Y. Deng, Spectrochim. Acta A 67 (2007) 1297.
[24] J. Matsui, H. Kubo, T. Takeuchi, Anal. Sci. 14 (1998) 699.
[25] M. Siemann, L.I. Andersson, K. Mosbach, J. Agric. Food Chem. 44 (1996) 141.
[26] M.L. Coote, D.J. Henry, Macromolecules 38 (2005) 1415.
[27] J. Chiefari, R.T.A. Mayadunne, C.L. Moad, G. Moad, E. Rizzardo, A. Postma, M.A. Skidmore, S.H. Thang, Macromolecules 36 (2003) 2273.
[28] A.R. Wang, S. Zhu, J. Polym. Sci.: Polym. Chem. 41 (2003) 1553.
[29] M.J. Monteiro, H. de Brouwer, Macromolecules 34 (2001) 349.
[30] E. Rizardo, J. Chiefari, Y.K. Chong, F. Ercole, J. Krstina, J. Jeffery, T.P.T. Le, Macromol. Symp. 143 (1999) 291.
[31] J. Matsui, Y. Miyoshi, O. Doblhoff-Dier, T. Takeuchi, Anal. Chem. 67 (1995) 4404.
[32] K. Yoshizako, K. Hosoya, Y. Iwakoshi, K. Kimata, N. Tanaka, Anal. Chem. 70 (1998) 386.